Density functional theory meta GGA study of water adsorption in MIL-53(Cr)

E. Cockayne [a)]
Materials Measurement Science Division, Material Measurement Laboratory, National Institute of Standards and Technology, Gaithersburg, Maryland 20899, USA

(Received 20 March 2019; accepted 20 June 2019)

We use density functional theory meta-generalized gradient approximation TPSS + D3(BJ) + U + J calculations to investigate the energetics and geometry of water molecules in the flexible metal-organic framework material Materials of Institut Lavoisier (MIL)-53(Cr) as a function of cell volume. The critical concentration of water to cause the transition from the large pore (*lp*) to the narrow pore (*np*) structure is estimated to be about 0.13 water molecule per Cr. At a concentration $x = 1$ water molecule per Cr, the zero-temperature *np* and *lp* configurations each have a hydrogen bond between the H of each framework hydroxyl group and water oxygen (O_W). At intermediate volumes, water dimer-like configurations are observed. A concentration $x = 1.25$ leads to hydrogen bonding between water molecules in the np phase that is absent for $x = 1$. Our results suggest possible mechanisms for pore closing in hydrated MIL-53(Cr). © *2019 International Centre for Diffraction Data.*
[doi:10.1017/S0885715619000587]

Key words: MIL-53(Cr), Hydrated MIL-53(Cr), MOFs, Water adsorption structures

I. INTRODUCTION

Flexible-framework nanoporous metal-organic materials are fascinating both from a fundamental point of view and for their potential applications such as gas storage, gas separation, sensors, etc. (Férey and Serre, 2009; Alhamami *et al*., 2014). A well-studied example is the Materials of Institut Lavoisier (MIL)-53(*M*) family (Serre *et al*., 2002) with formula $MC_8O_5H_5$, where *M* is a trivalent species such as Cr, Sc, Al, Ga or Fe (Figure 1). The structure formula can also be written as *M*(OH)(bdc), where bdc is the (1–4)benzodicarboxylate ion. Each metal ion *M* is octahedrally coordinated with six oxygens: four from carboxylate groups and two from hydroxyl groups. Zigzag *M*-OH-*M*-• • • chains are crosslinked by bdc ions to form a space-filling structure having linear pores with a diamond cross-section. These MIL-53(M) compounds typically exhibit both a narrow pore (*np*) and a large pore (*lp*) structure, with transitions between the two observed as a function of temperature, pressure, adsorption, etc.

The adsorption of water into metal-organic frameworks (MOFs) is a topic of great practical interest, as water affects the stability and gas sorption properties of MOFs operating in the atmosphere or in gas mixtures including water vapor (Burtch *et al*., 2014; Canivet *et al*., 2014; Furukawa *et al*., 2014). The MIL-53 family of flexible metal framework materials exhibits an interesting behavior on water absorption, typified by MIL-53(Cr). Dry MIL-53 is in the *lp* state. As the amount of water adsorption increases above some critical value, MIL-53(Cr) transitions to the *np* state. At sufficiently high loading, MIL-53(Cr) transitions back to the *lp* state (Bourrelly *et al*., 2010; Devautour-Vinot *et al*., 2010). This "breathing" behavior is typical of gas sorption in this family of flexible MOF materials.

The structure of water in MIL-53(Cr) has been studied from a variety of computational and experimental techniques (Llewellyn *et al*., 2008; Coombes *et al*., 2009; Dubbeldam *et al*., 2009; Salles *et al*., 2011; Cirera *et al*., 2012; Paesani, 2012; Haigis *et al*., 2013; Salazar *et al*., 2015). For the *np* phase at a loading of $x = 1$ H_2O per Cr, there is a strong consensus that each water oxygen, or O_W, forms a strong hydrogen bond with an H atom of an OH group of the framework. The water hydrogens (H_W) may participate in bonding with the framework O atoms or with the O_W of other water molecules, but there is less consensus on the details of these bonds. In a powder X-ray structure refinement, Guillou *et al*. (2011) found a split position for the O_W, which they interpreted as evidence for dimerization of consecutive O_W via hydrogen bonding.

Haigis *et al*. (2013) used *ab initio* molecular dynamics at the PBE + D2 (Perdew *et al*., 1996; Grimme, 2006) level to investigate the dynamic behavior of water molecules in MIL-53 (Cr) for concentrations $x = 1.0$ and $x = 6.0$. For $x = 1.0$, the *np* phase was stabilized, each O_W remained bound to an OH group via hydrogen bonding, and the H_W rotated freely around the dipole axes of the water molecules. For $x = 6.0$, the *lp* phase was stabilized, one O_W was (quasi)statically bound to each exposed hydroxyl group, while the remaining H_2O moved fluidly, although with slower dynamics than in bulk H_2O.

While most published density functional theory (DFT) works on molecular adsorption in MOFs to date have been performed at the generalized gradient approximation (GGA) level, it is known (Tran *et al*., 2016) that no GGA is excellent for both solids and molecules at the same time, precisely the cases for the MOF and adsorbate molecule, respectively. Tran *et al*. (2016) recommend the use of a meta-GGA (MGGA) density functional for cases involving "both finite and infinite systems". Additionally, as described in the next

[a)]Author to whom correspondence should be addressed. Electronic mail: eric.cockayne@nist.gov

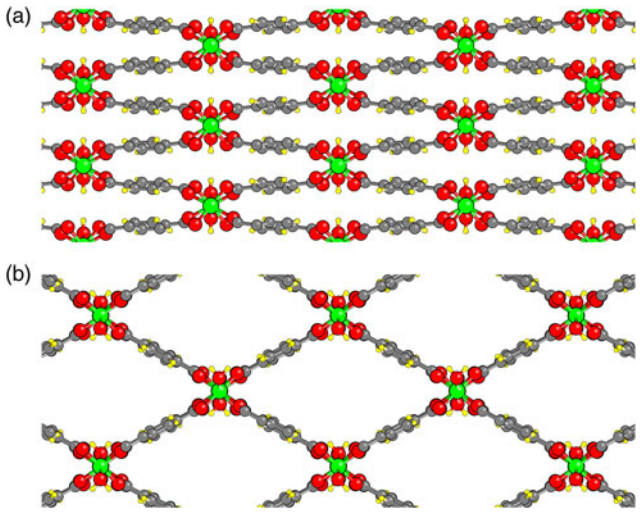

Figure 1. Structure of MIL-53(Cr) viewed down the *c*-axis. (a) Narrow pore (*np*) state; (b) Large pore (*lp*) state. Chromium atoms green; carbon gray; oxygen red and hydrogen yellow.

section, density functionals at the MGGA level perform better at describing interactions *between* water molecules than those at the GGA level. With the aim of developing a more accurate description of the geometry and energetics of water adsorption in MOFs, we use a MGGA density functional suitable for water in this work to investigate water adsorption in MIL-53 (Cr) for water concentrations of $x = 1.0$ and $x = 1.25$.

II. COMPUTATIONAL METHODS

First principles DFT calculations, as encoded in the VASP software (Kresse and Furthmuller, 1996), were used to calculate the relaxed configurations investigated here and their electronic structures. Certain commercial software is identified in this paper to adequately describe the methodology used. Such identification does not imply recommendation or endorsement by the National Institute of Standards and Technology, nor does it imply that the software identified is necessarily the best available for the purpose. Cells of composition $Cr_8O_{40}C_{64}H_{40}(H_2O)_{8x}$ were used for all calculations. The *c*-axis of the cells used were doubled with respect to that of the conventional cell. Lengthening the repeat distance in the open channels from around 7 Å to around 14 Å allows for a greater variety of water configurations to be studied. Monoclinic *np* MIL-53(Cr) has the space group *C2/c*, and orthorhombic *lp* MIL-53(Cr) has the space group *Imma*, but in this work we fixed the symmetry at the common subgroup $P2_1$ (space group 4) to maintain a monoclinic or higher-symmetry cell while allowing placement of water molecules such that they did not interfere with symmetry-equivalent versions of themselves. The parent *C2/c* or *Imma* symmetry is implicit in an ensemble of equal-energy configurations related by translation and other symmetry elements.

It is important to treat the interactions between water molecules properly in DFT calculations (Gillan *et al*., 2016). The widely used "PBE" (Perdew *et al*., 1996) GGA exchange correlation functional leads to overbonding between water molecules; that is the bonding energy is too high and the hydrogen bonding distances too short; a problem that is even worse when dispersion effects are considered (Santra *et al*., 2008). Instead, dispersion-corrected MGGA functionals are required to get the proper balance of forces necessary to accurately model water interactions (Pestana *et al*., 2017). In previous work (Cockayne and Nelson, 2015; Cockayne, 2017), we were able to reproduce benchmarking energies and geometries of small water clusters quite well by using a combination of a PBEsol (Perdew *et al*., 2008) gradient term, the RTPSS MGGA density functional (Perdew *et al*., 2009; Sun *et al*., 2011), empirical van der Waals forces at the Grimme D2 level (Grimme, 2006), and a Hubbard U value of 7.05 for the water oxygen, but the combination of parameters that we chose was admittedly *ad hoc* and not derived self-consistently. In this work, we seek a more transferable density functional, one that has been benchmarked across different systems in the literature. In this regard, we find that good agreement with benchmarking calculations on ice polymorph energies (Brandenburg *et al*., 2015), molecular clusters, and water clusters (Brandenburg *et al*., 2016) is obtained with the TPSS MGGA functional (Tao *et al*., 2003; Perdew *et al*., 2005) combined with empirical dispersion at the Grimme D3(BJ) level (Grimme *et al*., 2011). We note that the parameters of the D3(BJ) dispersion formula were optimized in Brandenburg *et al*. (2016) and use their TPSS + D3(BJ) parameterization here. As we did in Cockayne (2017), we determined Hubbard correction parameters U and J for Cr within the TPSS + D3(BJ) approach by attempting to fit the unit cell volume and bandgap of corundum Cr_2O_3. The optimal values found were $U = 2.7$ eV and $J = 1.7$ eV.

A $2 \times 2 \times 2$ Monkhorst-Pack k-point grid was used for all calculations. It was verified that calculated energies and forces were converged with respect to the number of k points. The planewave cutoff was 500 eV. In dry MIL-53(Cr), the Cr atoms were found to prefer high spin magnetic states with neighboring Cr in an antiferromagnetic arrangement (Cockayne, 2017); thus, this magnetic configuration was initialized for the structures studied in this work. Each atomic relaxation was performed at a fixed volume with the cell shape allowed to relax. The volume was varied in small increments to map the enthalpy vs. volume equation of state. In some cases, the water configuration of the MIL-53(Cr) + H_2O system spontaneously transformed into a different geometry. In these cases, the new geometry was taken as a starting point for a set of enthalpy vs. volume calculations until crossing points or transformation points between the different configurations were determined.

III. RESULTS

To benchmark our results based on the benchmarked dispersion-corrected MGGA, we first compare the enthalpy vs. volume of *dry* MIL-53(Cr) using the benchmarked MGGA functional with previous results (Cockayne, 2017) on MIL-53(Cr) that used the *ad hoc* MGGA functional described in the Methods section. The results are shown in Figure 2. For comparison with other results in the literature, one mole refers to one mole of $Cr_4O_{20}C_{32}H_{20}(H_2O)_{4x}$ throughout this work, and cell volumes are given for the "primitive" cell of this composition. Both sets of calculations have a minimum enthalpy for the *np* phase in contrast to experimental results showing that the *lp* phase is stable at all temperatures. In Cockayne (2017), this discrepancy was shown to arise from a combination of DFT error and the

https://doi.org/10.1017/S0885715619000587 Published online by Cambridge University Press

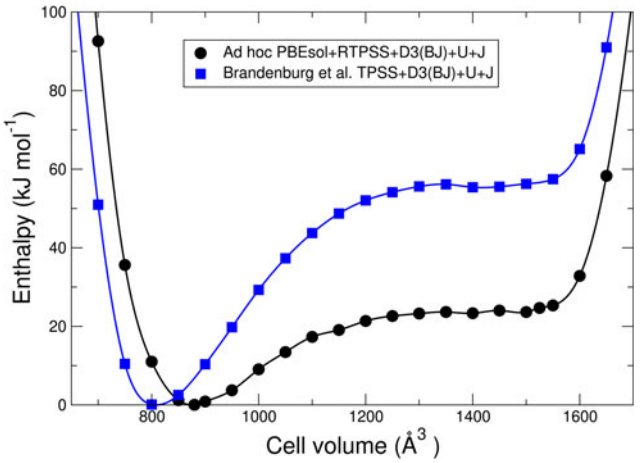

Figure 2. Comparison of enthalpy vs. volume of dry MIL-53(Cr) using an *ad hoc* parameterization of DFT at the MGGA level (PBEsol + RTPSS + D3(BJ) + U + J) (Cockayne and Nelson, 2015; Cockayne, 2017) and a MGGA that has been benchmarked across different systems (TPSS + D3(BJ) + U + J) (Brandenburg *et al.*, 2016).

neglect of vibrational enthalpy. By consideration of the relative phase stability of the *np* and *lp* structures, it is seen that the benchmarked MGGA functional actually performs *worse* for dry MIL-53(Cr) than the *ad hoc* one. Nonetheless, we use the benchmarked TPSS + D3(BJ) + U + J MGGA functional in this work because of its known transferability across different systems. One must keep in mind that the results of this work will tend to show overbinding of the *np* structure with respect to the *lp* one; but at fixed volume, one expects interactions involving water to be reasonably accurate.

Having established the quality of our density functional on dry MIL-53(Cr), we move to the interaction of MIL-53 (Cr) with water. We first present results for composition $x =$ 1.0 H_2O per Cr. Structures were initialized both in the *lp* phase and *np* phase. Given previous results, one O_W was set at a hydrogen bonding distance from the H of each hydroxyl group in the framework; the H positions of the water molecules were initially randomized. The exploration of structure vs. volume was performed as described in the Methods section. In all, five different configurations are found (Figure 3), whose calculated enthalpies as a function of volume are shown in Figure 4.

Four of the five configurations (I, II, IV,V) have all of the O_W hydrogen bonded to a framework H and one H_W of each H_2O forming a bond with a framework O on the same side of the pore. In the *np* state (configuration I), the pore becomes so narrow that the other H_W of each H_2O forms a bond with a framework O on the *opposite* side of the pore. The geometry at intermediate volumes (configuration III) is different. Consecutive pairs of water molecules along the pore dimerize. In doing so, some of the hydrogen bonds between O_W and the framework are broken. Inspection of the geometry of the water molecules in this dimer shows that it is very similar to that of an isolated water dimer. Note that the H_2O bonding arrangements at the top of the pore differ between configurations II and IV. Configurations IV and V differ subtly as can be observed by differences in the orientations of the H_W.

Note that the "dimer" configuration III interrupts what is essentially a smooth energy curve for each configuration with each O_W hydrogen bonded to the framework. The transition from configuration I to configuration II is not precisely

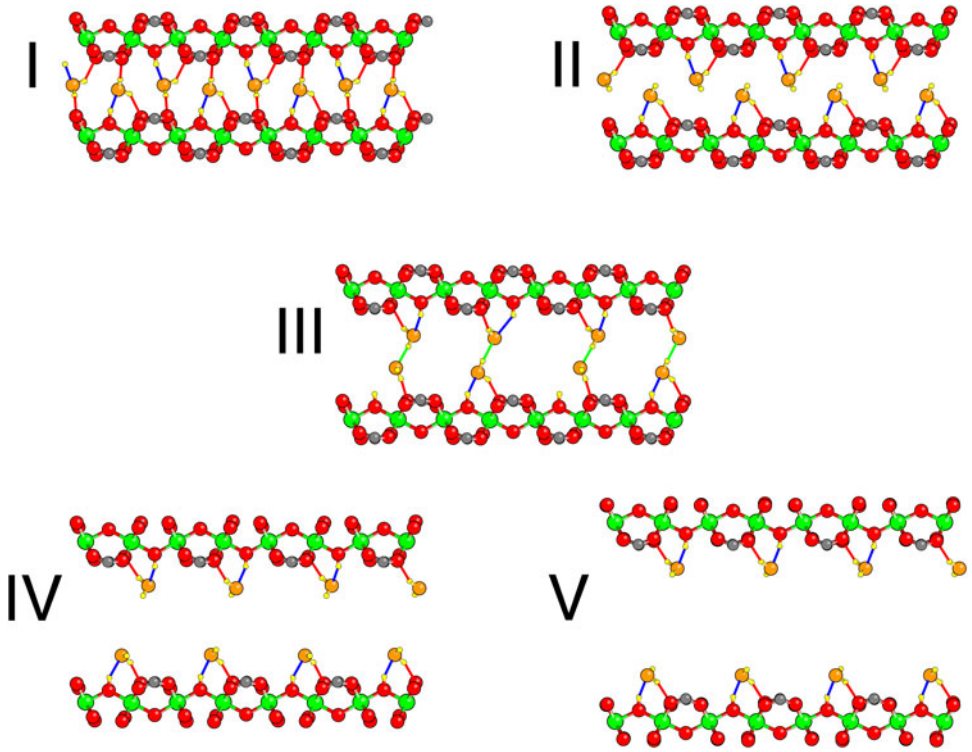

Figure 3. Five different relaxed configurations found during DFT studies of MIL-53 hydrated at $x = 1$, in order of increasing cell volume. In contrast to Figure 1, the view is down the *a*-axis, and the tunnel axis runs left–right. Cr atoms are green, framework O red, O_W orange and H yellow. O–H bonds, defined as O and H separated by <2.3 Å, are shown: hydrogen bonds between O_W and framework are blue, bonds between H_W and framework red, and hydrogen bonds between water molecules green.

https://doi.org/10.1017/S0885715619000587 Published online by Cambridge University Press

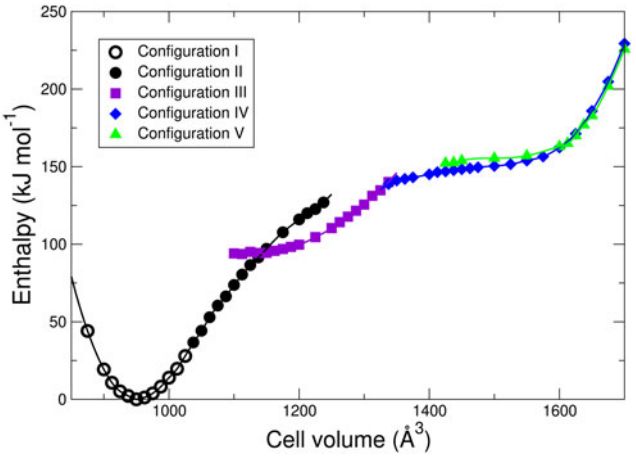

Figure 4. Energetics of H_2O adsorption in MIL-53 as a function of volume and configuration type shown in Figure 3.

defined because of continuous stretching of the O–H bonds across the pore, but occurs roughly at a cell volume roughly 1030 Å^3. The other transitions are between geometrically distinct configurations and the transition volumes can thus be defined as those at which the enthalpies cross: II–III at 1144 Å^3; III–IV at 1331 Å^3, and IV–V at 1604 Å^3. As the volume decreases, the DFT relaxation of configuration V spontaneously transforms into configuration IV at a cell volume of about 1400 Å^3; while upon expansion configuration IV remains metastable until at least cell volume 1725 Å^3. The dimer of configuration III spontaneously breaks up into the separate water molecules into configuration IV and vice versa at a volume not far from the equilibrium volume. Configurations II and III remain metastable up to at least the volumes shown in Figure 4.

For $x = 0$, the calculated enthalpy difference between the *np* and *lp* phases is 55 kJ mol^{-1}. For $x = 1$, the difference is approximately 150 kJ mol^{-1}. While our results incorrectly predict the *np* phase to be more stable, the experimental free energy of the *lp* phase of MIL-53(Cr) is approximately 12 kJ mol^{-1} lower than that of the *np* phase at room temperature (Coombes *et al.*, 2009; Coudert *et al.*, 2008; Devautour-Vinot *et al.*, 2009; Beurroies *et al.*, 2010). Assuming that the enthalpy difference change of 95 kJ mol^{-1} from $x = 0$ to $x = 1$ is correctly computed by the DFT calculations, that this change is linear in composition, and that changes in free energy can be approximated by changes in enthalpy, we estimate that the transition from the *lp* phase to the *np* phase in hydrated MIL-53(Cr) will occur at a composition near $x = 0.13$.

While Guillou *et al.* (2011) reported evidence for hydrogen-bound water dimers in *np* MIL53(Cr), our results showed dimers only at intermediate volumes. We thus performed further explorations of water in the *np* phase. Note that the average O_W–O_W separation distance along a tunnel in MIL-53(Cr) is about 3.4 Å, which is not a favorable distance for hydrogen bonding. We note, however, that the doubled MIL-53(Cr) *c* lattice parameter of about 13.6 Å that we use in this study could accommodate 5 H_2O per repeat distance with favorable O_W–O_W distances for hydrogen bonding. This led us to study the relaxed geometries of *np* MIL-53(Cr) with $x = 1.25$ H_2O per Cr.

Five H_2O molecules were initially placed in the MIL-53 (Cr) *np* structure such that an O_W and H_W of each H_2O were along the central axis of the tunnel with each H_W pointing toward the O_W of the next molecule [Figure 5(b)]. One water molecule had its other H_W in the *ac* plane. The other water hydrogens were successively rotated by an angle of $2\pi/5$. With this arrangement, not only is there a hydrogen bond between each successive pair of water molecules, but each hydroxyl unit forms a hydrogen bond with one water molecule, and there are some additional bonds between H_W and carboxylate oxygens as in the $x = 1$ case.

We first relax the $x = 1.25$ structure with the constraint that the O_W and H_W originally involved in the hydrogen bonding remain along the tunnel axis. The results are shown in Figure 5(c). Note that one interwater hydrogen bond is broken to improve interactions with the framework. We then perform a full relaxation. In the full relaxation [Figure 5(d)], a different hydrogen bond is broken, and water molecules show noticeable displacement from the central axis. Our results predict that the number of intermolecular H bonds in hydrated MIL-53(Cr) should dramatically increase as the composition is raised above $x = 1$.

IV. DISCUSSION

Throughout the text, we have been careful to use the term "hydrogen bond" to describe bonding between water

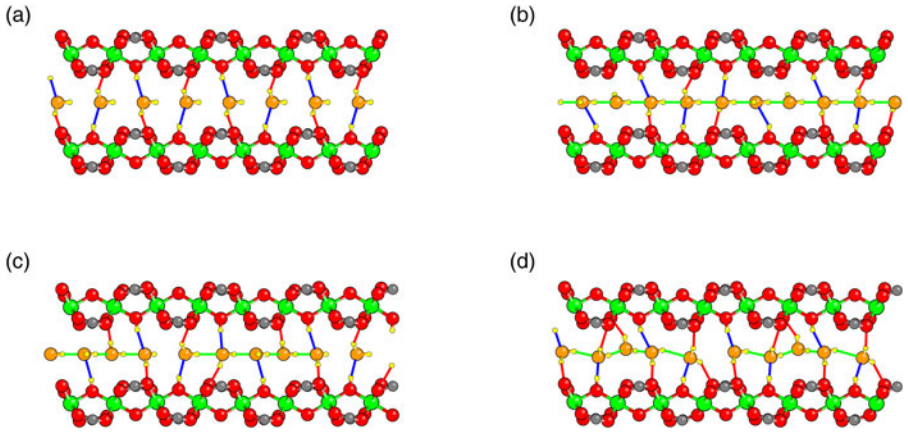

Figure 5. Hydrogen bonding between water molecules in and configuration type. (a) Average separation of 4 H_2O per repeat distance is too long for hydrogen bonding. (b) Initialization of structure with 5 H_2O per repeat distance. (c) Constrained relaxation. (d) Full relaxation.

https://doi.org/10.1017/S0885715619000587 Published online by Cambridge University Press

molecules and binding of a water oxygen O_W to the H of the hydroxyl unit of the MIL-53(Cr) framework. On the other hand, we have simply used the term "bond" to describe the interaction between water hydrogens H_W and carboxylate oxygens, even though the species involved are the same and separation distances are similar in both cases. We base our terminology on the *ab initio* molecular dynamics results of Haigis *et al*. (2013), where they find that the H_W–carboxylate oxygen interactions are not true hydrogen bonds, because (at the 350 K simulation temperature), the interaction of a H_W with an individual carboxylate atom had only a short lifetime (typically <200 fs). Our results are essentially zero temperature results ignoring zero-point vibrational motion. Under these conditions, the minimum energy configurations do show H_W bonded to carboxylate oxygens at a typical distance of about 1.8 Å to 1.9 Å typical of hydrogen bonding. It would be interesting to calculate the shape and depth of this binding well in comparison with the zero-point vibrational energy of an H_W in this well to see if the H is truly bound at zero temperature.

Guillou *et al*. (2011) used structure refinement results showing a split O_W position to conclude that water dimers formed in *np* MIL-53(Cr). Our results present an alternate interpretation. In configuration I of Figure 3, the H_2O with O_W bound to the bottom of the pore tilt to the right. To reproduce the parent *C2/c* symmetry, equivalent configurations with the H_2O tilted to the left must be included. Supposing that an actual *np* structure has a statistical mix of these configurations locally, then the average crystallographic structure would have a split O_W position. The difference between the O_W position of our symmetrized configuration I with the O_W position in the Supplementary Material of Guillou *et al*. (2011) is only 0.2 Å. We conclude that the split O_W position seen in the crystallographic refinement does not necessarily imply that the water molecules form dimers.

The energetics of the global water configurations shown in Figure 3 have interesting implications if they apply to local pore closing dynamics in MIL-53(Cr). The results imply that, as H_2O is added to the *lp* structure of dry MIL-53(Cr), H_2O attached to consecutive OH units on opposite sides of the pore could attract each other to form a dimer, first accelerating the pore closing as seen in the energy vs. volume curve of configuration III (Figure 4). However, the energy barrier between configuration III and configuration IV that is implied by the metastability of each of these configurations into the volume domain of the other suggests that complete closing of the pore is somewhat hindered.

V. CONCLUSIONS

The energetics of water adsorption into MIL-53(Cr) was investigated using DFT at the MGGA level. Various types of important O–H interactions were identified. At 1.0 H_2O per Cr, for volumes intermediate between those of the *np* and *lp* structures, a low-energy configuration was found where all water molecules are paired into dimers. Our results provide a basis for the interpretation of experimental, theoretical and modeling work on water adsorption up to 1.25 H_2O per Cr.

Alhamami, M., Doan, H., and Chen, C.-H. (**2014**). "A review of breathing behaviors of MOFs for gas adsorption," *Materials (Basel)* **7**, 3198–3250.

Beurroies, I., Boulhout, M., Llewellyn, P. L., Kuchta, B., Férey, G., Serre, C., and Denoyel, R. (**2010**). "Using pressure to provoke the structural transition of metal-organic frameworks," Angew. Chem. Int. Ed. **49**, 7526–7529.

Bourrelly, S., Moulin, B., Rivera, A., Maurin, G., Devautour-Vinot, S., Serre, C., Devic, T., Horcajada, P., Vimont, A., Clet, G., Daturi, M., Lavalley, J.-C., Loera-Serna, S., Denoyel, R., Llewellyn, P. P., and Férey, G. (**2010**). "Explanation of the adsorption of polar vapors in the highly flexible metal organic framework MIL-53(Cr)," J. Am. Chem. Soc. **132**, 9488–9498.

Brandenburg, J. G., Maas, T., and Grimme, S. (**2015**). "Benchmarking DFT and semiempirical methods on structures and lattice energies for ten ice polymorphs," J. Chem. Phys. **142**(12), 124104.

Brandenburg, J. G., Bates, J. E., Sun, J., and Perdew, J. P. (**2016**). "Benchmark tests of a strongly constrained semilocal functional with a long-range dispersion correction," Phys. Rev. B **94**(11), 115144.

Burtch, N. C., Jasuja, H., and Walton, K. S. (**2014**). "Water stability and adsorption in metal-organic frameworks," Chem. Rev. **114**, 10575–10162.

Canivet, J., Fateeva, A., Guo, Y., Coasne, B., and Farrusseng, D. (**2014**). "Water adsorption in MOFs: fundamentals and applications," Chem. Soc. Rev. **43**, 5594–5617.

Cirera, J., Sung, J. C., Howland, P. B., and Paesani, F. (**2012**). "The effects of electronic polarization on water adsorption in metal-organic frameworks: H_2O in MIL-53(Cr)," J. Chem. Phys. **137**, 054704.

Cockayne, E. (**2017**). "Thermodynamics of the flexible metal–-organic framework material MIL-53(Cr) from first-principles," J. Phys. Chem. C **121** (8), 4312–4317.

Cockayne, E., and Nelson, E. B. (**2015**). "Density functional theory meta-GGA plus U study of water incorporation in the metal-organic framework material Cu-BTC," J. Chem. Phys. **143**, 024701.

Coombes, D. S., Corà, F., Mellot-Draznieks, C., and Bell, R. G. (**2009**). "Sorption-induced breathing in the flexible metal organic framework CrMIL-53: force field simulations and electronic structure analysis," J. Phys. Chem. C **113**, 544–552.

Coudert, F.-X., Jeffroy, M., Fuchs, A. H., Boutin, A., and Mellot-Draznicks, C. (**2008**). "Thermodynamics of guest-induced structural transitions in hybrid organic-inorganic frameworks," J. Am. Chem. Soc. **130**, 14294–14302.

Devautour-Vinot, S., Maurin, G., Henn, F., Serre, C., Devic, T., and Férey, G. (**2009**). "Estimation of the breathing energy of flexible MOFs by combining TGA and DSC techniques," Chem. Commun. (19), 2733–2735.

Devautour-Vinot, S., Maurin, G., Henn, F., and Serre, C. (**2010**). "Water and ethanol desorption in the flexible metal-organic frameworks MIL-53 (Cr, Fe), investigated by complex impedance spectroscopy and density functional theory calculations," Phys. Chem. Chem. Phys. **12**, 12748–12485.

Dubbeldam, D., Krishna, R., and Snurr, R. Q. (**2009**). "Method for analyzing structural changes of flexible metal- organic frameworks induced by adsorbates," J. Phys. Chem. C **113**, 19317–19327.

Férey, G., and Serre, C. (**2009**). "Large breathing effects in three-dimensional porous hybrid matter: facts, analyses, rules, and consequences," Chem. Soc. Rev. **38**, 1380–1399.

Furukawa, H., Gándara, F., Zhang, Y.-B., Jiang, J., Queen, W. L., Hudson, M. R., and Yaghi, O. M. (**2014**). "Water adsorption in porous metal-organic frameworks and related materials," J. Amer. Chem. Soc. **136**, 4369–4381.

Gillan, M. J., Alfè, D., and Michaelides, A. (**2016**). "Perspective: how good is DFT for water?," J. Chem. Phys. **144**(13), 130901.

Grimme, S. (**2006**). "Semiempirical GGA-type density functional constructed with a long-range dispersion correction," J. Computat. Chem. **27**, 1787–1799.

Grimme, S., Ehrlich, S., and Goerigk, L. (**2011**). "Effect of the damping function in dispersion corrected density functional theory," J. Computat. Chem. **32**, 1456–1465.

Guillou, N., Millange, F., and Walton, R. I. (**2011**). "Rapid and reversible formation of a crystalline hydrate of a metal-organic framework containing a tube of hydrogen-bonded water," Chem. Commun. **47**, 713–715.

Haigis, V., Coudert, F.-X., Vuilleumier, R., and Boutin, A. (**2013**). "Investigation of structure and dynamics of the hydrated metal-organic framework MIL-53(Cr) using first-principles molecular dynamics," Phys. Chem. Chem. Phys. **15**, 19049–19055.

Kresse, G., and Furthmuller, J. (**1996**). "Efficient iterative schemes for *ab initio* total-energy calculations using a plane-wave basis set," Phys. Rev. B **54**, 11169–11187.

https://doi.org/10.1017/S0885715619000587 Published online by Cambridge University Press

Llewellyn, P. L., Maurin, G., Devic, T., Loera-Serna, S., Rosenbach, N., Serre, C., Bourrelly, S., Horcajada, P., Filinchuk, Y., and Férey, G. (**2008**). "Prediction of the conditions for breathing of metal organic framework materials using a combination of x-ray powder diffraction, microcalorimetry and molecular simulation," J. Am. Chem. Soc. **130**, 12808–12814.

Paesani, F. (**2012**). "Water in metal-organic frameworks: structure and diffusion of H_2O in MIL-53(Cr) from quantum simulations," Mol. Simul. **38**, 631–641.

Perdew, J. P., Burke, K., and Ernzerhof, M. (**1996**). "Generalized gradient approximation made simple," Phys. Rev. Lett. **77**, 3865–3868.

Perdew, J. P., Ruzsinszky, A., Tao, J., Staroverov, V. N., Scuseria, G. E., and Csonka, G. I. (**2005**). "Prescription for the design and selection of density functional approximations: more constraint satisfaction with fewer fits," J. Chem. Phys. **123**, 062201.

Perdew J., Ruzsinszky A., Csonka G. I., Vydrov O. A., Scuseria G. E., Constantin L. A., Zhou X., and Burke K. (**2008**). "Restoring the density-gradient expansion for exchange in solids and surfaces," Phys. Rev. Lett. **100**, 136406.

Perdew, J. P., Ruzsinszky, A., Csonka, G. I., Constantin, L. A., and Sun, J. (**2009**). "Workhorse semilocal density functional for condensed matter physics and quantum chemistry," Phys. Rev. Lett. **103**(2), 026403.

Pestana, L. R., Mardirossian, N., Head-Gordon, M., and Head-Gordon, T. (**2017**). "Ab initio molecular dynamics simulations of liquid water using high quality meta-GGA functionals," Chem. Sci. **8**(5), 3554–3565.

Salazar, J. M., Weber, G., Simon, J. M., Bezverkhyy, I., and Bellat, J. P. (**2015**). "Characterization of adsorbed water in MIL-53(Al) by FTIR spectroscopy and ab-initio calculations," J. Chem. Phys. **142**, 124702.

Salles, F., Bourrelly, S., Jobic, H., Devic, T., Guillerm, V., Llwewllyn, P., Serra, C., Férey, G., and Maurin, G. (**2011**). "Molecular insight into the absorption and diffusion of water in the versatile hydrophilic/hydrophobic flexible MIL-53(Cr) MOF," J. Phys. Chem. C **115**, 10764–10776.

Santra, B., Michaelides, A., Fuchs, M., Tkatchenko, A., Filippi, C., and Scheffler, M. (**2008**). "On the accuracy of density-functional theory exchange-correlation functionals for H bonds in small water clusters. II. the water hexamer and van der Waals interactions," J. Chem. Phys. **129**(19), 194111.

Serre, C., Millange, F., Thouvenot, C., Noguès, M., Marsolier, G., Louër, D., and Férey, G. (**2002**). "Very large breathing effect in the first nanoporous Chromium-III based solids: MIL53 or ….," J. Am. Chem. Soc. **124**, 13519–13526.

Sun, J., Marsman, M., Csonka, G., Ruzsinszky, A., Hao, P., Kim, Y.-S., Kresse, G., and Perdew, J. P. (**2011**). "Self-consistent meta-generalized gradient approximation within the projector-augmented-wave method," Phys. Rev. B **84**, 035117.

Tao, J., Perdew, J. P., Staroverov, V. N., and Scuseria, G. E. (**2003**). "Climbing the density functional ladder: nonempirical meta–generalized gradient approximation designed for molecules and solids," Phys. Rev. Lett. **91**(14), 146401.

Tran, F., Stelzl, J., and Blaha, P. (**2016**). "Rungs 1 to 4 of DFT Jacob's ladder: extensive test on the lattice constant, bulk modulus, and cohesive energy of solids," J. Chem. Phys. **144**, 204120.

https://doi.org/10.1017/S0885715619000587 Published online by Cambridge University Press